Robust Model Predictive Control for Robot Manipulators

S. Mohammad Tahamipour-Z., Member, IEEE, Goran R. Petrovic and Jouni Mattila

Abstract— **Inherent nonlinearities, external disturbances and model uncertainties hinder the performance of controlling real-world systems. In the present study, we proposed a robust model prediction-based virtual decomposition control method (RMP-VDC) as a modification of the VDC using the model predictive control (MPC) to offer a practical solution for the real system control problem. The proposed method deals with uncertainties and external forces, as well as constraint matters, for complex nonlinear robot manipulators. By modifying the ideas from the VDC with MPC techniques, the time-varying state feedback control law for the ancillary controller is provided. The proposed method benefits from the introduction of a prediction horizon, which induces robustness and increases accuracy. The constrained optimization problem is analytically solved online by the continuous linearization of the nonlinear model and by employing the active set method. To validate the proposed controller, we performed the implementation on a real 7-degrees-of-freedom upper body exoskeleton robot, and the results were compared with those obtained using the adaptive VDC. The experimental results revealed increased accuracy for the proposed RMP-VDC in dealing with model uncertainties and interaction forces between humans and exoskeleton robots.**

I. Introduction

Modelling complexity, external disturbances, and inherent nonlinearities of real-world systems make dynamics models inaccurate and present evident challenges for system control. Various control methods are presented and developed to deal with these challenges. For instance, computed torque control is introduced in [1] for considering structured and unstructured uncertainties in manipulators and has provided satisfactory results. In [2], an adaptive control is offered based on an artificial neural network to deal with uncertainties in friction models. An adaptive sliding mode control is presented in [3] to considerably guarantee the fast convergence of system outputs toward balancing and reducing the chattering issues. In [4], a fuzzy system-based sliding mode control is proposed whose benefits are both reducing computational costs and improving uncertainty handling for the modelling and control of nonlinear systems.

Furthermore, to deal with uncertainties and reduce conservatism simultaneously, an adaptive control based on model reference has been developed [5]. Although, weak performance at the start of adaptation and slow convergence are challenges of the model reference adaptive control. In [5], a new method for adaptive control based on model reference and the normalised Lyapunov strategy is proposed to avoid oscillatory response and to reach quick convergence.

The control of interaction forces between humans and systems is the main challenge of other studies. For example, the proportional derivative and neural network-based biological controller in [6], computed torque control in [7], output feedback assistive controller in [8], an assist-as-needed control based on a new strength index in [9] and real-time model predictive control (MPC) [10] are proposed to control the interaction force between patients and exoskeleton robots.

However, these controllers are designed for systems with a small number of degrees of freedom (DoF) (e.g. two-link elbow planar manipulator [1]; 2-DoF [2] and 4-DoF SCARA robot [5]; 2-DoF forearm and wrist rehabilitation robot [3]; 3-DoF parallel robot [4]; 3-DoF arm exoskeletons robot [6]; 4-DoF orthosis [7]; 1-DoF knee exoskeleton [8]; 2-DoF hip exoskeleton [9]; and 2-DoF lower limb exoskeleton [10]). Therefore, control methods are now being developed to overcome the challenges in highly complex robot systems, e.g., exoskeleton robots with higher number of DoF and system variability, due to the interaction force between the system and environment. In [11], a review of the challenges in the 7-DoF exoskeleton is presented to improve functionality. In addition, a time-delay estimator-based adaptive tracking control is proposed in [12] to deal with uncertain dynamics, and an adaptive impedance control with backstepping approach, disturbance observer, and time-delay estimation methods is presented in [13] to deal with unknown torque disturbances.

In [14], a virtual decomposition control (VDC) approach is proposed, which provides a computationally effective solution for precision model-based control with practically proven capabilities in handling complex robotic systems [15, 16]. The kinematics and dynamics modelling [17], the control forming, and stability analysis all rely heavily on the modularity property, which is perceived as the main property required in future industrial innovations for handling complexity [18]. Control actions in the VDC mostly rely on feed-forward forces/moments, which are generated with inverse dynamical calculations. Also, feedback is considered to provide stability, to secure smooth transitions, and to deal with model parameter uncertainties.

Moreover, control values are formed on a subsystem level, where making physical or mathematical changes regarding one subsystem does not affect the control equations for the rest of the system. Care is also taken to rigorously maintain the L_2 and L_∞ stability of the total robot manipulator systems. In a virtually partitioned system, the dynamic interactions between subsystems mathematically are handled by the VDC methods

*Research supported by the Technology Industries of Finland Centennial Foundation and the Jane and Aatos Erkko Foundation Future Makers programme.

S. Mohammad Tahamipour-Z. (corresponding author), Goran R. Petrovic, and Jouni Mattila are with the Automation Technology and Mechanical Engineering Unit in the Faculty of Engineering and Natural Sciences at Tampere University, Tampere, Finland
(Email : seyedmohammad.tahamipourzarandi@tuni.fi).

through the virtual power flows [17]. The two adjacent virtual subsystems have the opposite signed virtual power flow with the same magnitude, which adds up to zero in the stability analysis, which is how stability analysis benefits from modularity [14]. Problem of the model complexity is also kept constant, indicating that by increasing the DoF of the robot, the total complexity also rises exponentially. To account for the facilitation of implementing a 7-DoF robot, as well as to deal with dynamics variability resulting from different biomechanical and physiological factors in patients, [19] presents a VDC approach to deal with model parameter uncertainties such as stiffness of the joints, different masses, and various user with biomechanical variations while model uncertainties, external disturbances, and constraints of actuators are not considered.

By contrast, the MPC methods have also been widely used in the industrial fields, and results show the performance superiority of the MPC due to its prediction and optimization in controlling multivariable systems and handling hard constraints for complex industry systems [20]. The main challenge of the MPC method, however, is the computational burden for solving the nonlinear optimization problem which grows exponentially when system uncertainty is involved. Thus, the real-time implementation of the MPC scheme is the main challenge of this method since the optimization problem for nonlinear systems needs to be solved and the cost of prediction for systems is time. Because of the efforts made by researchers, real-time frameworks for MPC have been proposed in recent years [10, 21, 22] and have been employed as control methods in robotic applications such as lower limb exoskeleton robots [10], mobile robots [21] and humanoids [22]. In addition, robust tube-based MPC methods have been developed and presented for other applications such as industrial robots [23], mobile robots [24], and humanoids [25] to deal with model uncertainties and external disturbances.

Here, inspired from the above, we proposed a robust model predictive (RMP)-VDC method. The proposed controller benefits from the advantages of the MPC and VDC methods to deal with inherent nonlinearity, model uncertainties and external disturbances as well as input saturations for complex systems. To the best of our knowledge, the VDC method is not yet equipped with tools to overcome these challenges. Given the real-time implementation of the RMP-VDC, the constrained optimisation problem is solved online by the linearisation of the nonlinear model and employing the active set method. The analytical solution to the problem is then obtained, and the real-time implementation of our approach is achieved by calculating the greatest number of mathematical processes required for an arbitrary prediction horizon. For validation, the proposed RMP-VDC method is implemented on a commercial 7-DoF upper body exoskeleton robot called ABLE by Haption Co. (www.haption.com). The results are compared with the adaptive VDC in [14]. The main contributions of this study can be summarised as follows:

1. A new RMP-VDC method that benefits from both the prediction and modelling of complex systems is proposed.
2. The robustness of the proposed controller is then guaranteed to deal with inherent nonlinearities and dynamics model uncertainties.
3. An analytical solution is offered for the optimisation problem, enabling real-time implementation.
4. The proposed method is implemented on a real complex 7-DoF upper body exoskeleton robot.

This paper is prepared as follows: section II describes the mathematical preliminaries; section III presents the proposed robust model prediction-based VDC method; section IV includes the experimental results of the proposed method on a real exoskeleton robot; and finally, section V shows the conclusions.

II. Mathematical Preliminaries

In this section, summary of the mathematical preliminaries used for the next section is presented. By reviewing [14], an orthogonal coordinate system (i.e. a frame) $\{S_1\}$ attached to a rigid body is first considered. The force/moment vector ${}^{S}F \in R^6$ and the linear/angular velocity vector ${}^{S}V \in R^6$ of the rigid body, as demonstrated in frame $\{S_1\}$, is:

$$ {}^{S_1}V = \begin{bmatrix} {}^{S_1}v \\ {}^{S_1}\omega \end{bmatrix} \text{ and } {}^{S_1}F = \begin{bmatrix} {}^{S_1}f \\ {}^{S_1}m \end{bmatrix}, \tag{1} $$

where ${}^{S_1}v \in R^3$ and ${}^{S_1}\omega \in R^3$ are the linear and angular velocity vectors of frame $\{S_1\}$, respectively; and ${}^{S_1}f \in R^3$ is the force and ${}^{S_1}m \in R^3$ is the moment vectors that are presented in frame $\{S_1\}$. By considering ${}^{S_1}U_{S_2} \in R^{6\times 6}$ as a force/moment transformation matrix, the force/moment and linear/angular velocity vectors can be transformed between $\{S_1\}$ and $\{S_2\}$ frames as follows:

$$ {}^{S_2}V = {}^{S_1}U_{S_2}^{T}\,{}^{S_1}V \text{ and } {}^{S_1}F = {}^{S_1}U_{S_2}\,{}^{S_2}F, \tag{2} $$

Then, the rigid body dynamics for frame $\{S_1\}$ is:

$$ M_{S_1}\,{}^{S_1}\dot{V} + C_{S_1}\,{}^{S_1}V + G_{S_1} = {}^{S_1}F^{*}, \tag{3} $$

where $G_{S_1} \in R^6$ denotes the gravity vector, $M_{S_1} \in R^{6\times 6}$ indicates the mass matrix, $C_{S_1} \in R^{6\times 6}$ is the matrix of the Coriolis and centrifugal terms, and ${}^{S_1}F^{*} \in R^6$ is the net force/moment vector. For a detailed formulation of M_{S_1}, C_{S_1} and G_{S_1}, see [14].

III. Robust Model Predictive-Based VDC

The overall structure of the proposed robust model prediction-based VDC is depicted in Fig. 1. A system–environment with an interaction force is considered. Thus, the dynamics equation of the system according to the VDC method is:

$$ M_s\,{}^{s}\dot{V} + C_s\,{}^{s}V + G_s = {}^{s}F - {}^{s}\bar{F}, \tag{4} $$

where ${}^{s}F \in R^6$ and ${}^{s}\bar{F} \in R^6$ are the force/moment vector in the frame {S} and the interaction/external forces expressed in frame {S}, respectively. In other words, ${}^{s}F$ and ${}^{s}\bar{F}$ are the control signal and external disturbances, respectively. As shown in Figure 1, the dynamics equation for the real system can be rewritten as:

$$ {}^{s}\dot{V} = M_s^{-1}(-C_s\,{}^{s}V + {}^{s}F - {}^{s}\bar{F} - G_s). \tag{5} $$

The control signal for each joint can be considered as:

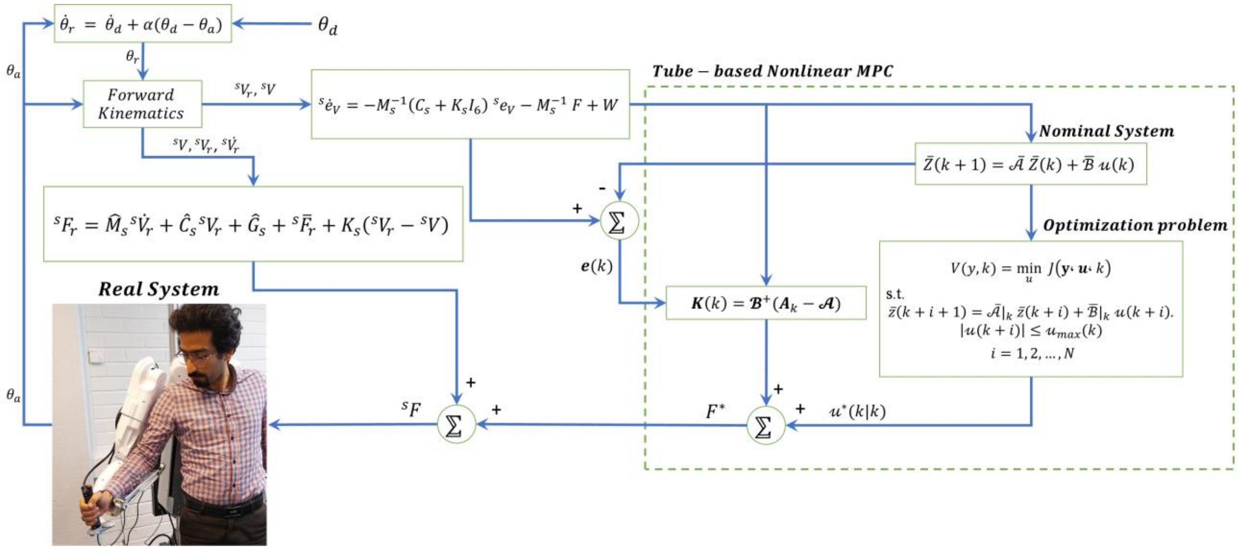

Figure 1. The overall structure of the proposed robust model prediction-based virtual decomposition.

$$ {}^sF = {}^sF_r + F^* = \hat{M}_s {}^s\dot{V}_r + \hat{C}_s {}^sV_r + \hat{G}_s + {}^s\bar{F}_r + K_s({}^sV_r - {}^sV) + F^*, \tag{6} $$

where F^* is the signal control from the MPC method, and $\hat{M}_s$, $\hat{C}_s$ and $\hat{G}_s$ matrices are the approximation matrices of the M_s, C_s and G_s, respectively. In addition, ${}^sF_r$ and ${}^sV_r$ are the required force and velocity, respectively. In the VDC framework, the required velocity is an important notion, and note that it is different from the desired velocity [17]. The required velocity is:

$$ \dot{\theta}_r = \dot{\theta}_d + \alpha\,(\theta_d - \theta_a), \tag{7} $$

where $\dot{\theta}_d$ is desired velocity and α is a positive constant. Also, θ_d and θ_a are the desired and actual positions of the joint, respectively. By replacing the ${}^sF$ in (5), we have:

$$ {}^s\dot{V} = -M_s^{-1}C_s{}^sV + M_s^{-1}\hat{M}_s{}^s\dot{V}_r + M_s^{-1}\hat{C}_s{}^sV_r + M_s^{-1}(F^*) + M_s^{-1}K_s({}^sV_r - {}^sV) + M_s^{-1}({}^s\bar{F}_r - {}^s\bar{F}) + M_s^{-1}(\hat{G}_s - G_s). \tag{8} $$

By adding the $\pm{}^s\dot{V}_r$ and $\pm M_s^{-1}\hat{C}_s{}^sV$ and considering the ${}^se_V = {}^sV_r - {}^sV$, we have:

$$ {}^s\dot{e}_V = -M_s^{-1}(C_s + K_sI_6)\,{}^se_V - M_s^{-1}\,(F^*) + W, \tag{9} $$

where:

$$ W = M_s^{-1}\big[(M_s - \hat{M}_s){}^s\dot{V}_r + (C_s - \hat{C}_s){}^sV + (G_s - \hat{G}_s) + ({}^s\bar{F} - {}^s\bar{F}_r)\big]. \tag{10} $$

The discrete-time system is:

$$ X(k+1) = A\,X(k) + B\,u(k) + \widetilde{W}, \tag{11} $$

where:

$$ X(k) = {}^se_V(k), \tag{12} $$

$$ u(k) = F^*, \tag{13} $$

$$ A = I_6 - \Delta t M_s^{-1}(C_s + K_sI_6), \tag{14} $$

$$ B = -\Delta t\, M_s^{-1}, \tag{15} $$

$$ \widetilde{W} = \Delta t W, \tag{16} $$

where Δt is the sampling time. A and B have parametric uncertainties such that the function $\rho(x) \coloneqq (A, B)$ can take any value in the convex set $P(x)$ at any time k, where:

$$ P(\boldsymbol{x}) \coloneqq co(A\,, B)\ |j \in \mathcal{L}, \tag{17} $$

with $\mathcal{L} \coloneqq 1,2, \dots, \mathcal{J}$ where $co(\cdot)$ specifies the convex hull set, and $\mathcal{J}$ is the corner number of the polytopic P. The nominal system is defined as:

$$ Z(k+1) = \mathcal{A}\,Z(k) + \mathcal{B}\,u(k), \tag{18} $$

where $u(k)$ is the input of the nominal system, and

$$ \mathcal{A} = \frac{1}{\mathcal{J}}\sum_{j=1}^{\mathcal{J}} A_j, \text{ and } \mathcal{B} = \frac{1}{\mathcal{J}}\sum_{j=1}^{\mathcal{J}} B_j. \tag{19} $$

Hence, (11) is rewritten as

$$ x(k+1) = \mathcal{A}\,x(k) + \mathcal{B}\,u(k) + \mathcal{W}(k), \tag{20} $$

where:

$$ \mathcal{W}(k) \coloneqq (A - \mathcal{A})x(k) + (B - \mathcal{B})u(k) + \widetilde{W}, \tag{21} $$

and $\mathcal{W} \in \overline{\mathbb{W}}$.

Assumption 1 (Boundedness of the uncertainty set $\overline{\mathbb{W}}$). Presumably, the uncertainty set $\overline{\mathbb{W}}$ is a compact bounded set that holds the origin.

Therefore, the ancillary control law can be defined as:

$$ u(k) = u(k) + K(k)(X(k) - Z(k)), \tag{22} $$

where $X(k)$ is the current state of the actual system, $Z(k)$ is the current state of the nominal system, and $K(k)$ is a time-varying state feedback matrix. Therefore, the closed-loop system dynamic is:

$$ \boldsymbol{x}(k+1) = A\,\boldsymbol{x}(k) + B\,u(k) + B\,K(k)e(k) + \mathcal{W}, \tag{23} $$

where

$$e(k) \coloneqq x(k) - z(k) \tag{24}$$

is the state error, with the following dynamics equation:

$$\begin{aligned} e(k+1) &= \big(\mathcal{A} + \mathcal{B}\,K(k)\big)e(k) + \mathcal{W} \\ &\coloneqq \bar{F}_k(z(k))e(k) + \mathcal{W}. \end{aligned} \tag{25}$$

Therefore, we obtained the following:

$$\begin{aligned} e(k) &= e(0)\textstyle\prod_{i=0}^{k-1}\bar{F}_i(z(k)) + \\ &\textstyle\sum_{j=0}^{k-1}\big(\mathcal{W}(j)\prod_{i=j+1}^{k-1}\bar{F}_i(z(k))\big). \end{aligned} \tag{26}$$

By setting $x(0) = z(0)$, we have $e(0) = 0$. Now, the controller gain is set as:

$$K(k) = \mathcal{B}^{+}(A_k - \mathcal{A}), \tag{27}$$

where A_k is a positive stable matrix, and $\mathcal{B}^{+}$ indicates the pseudoinverse of the matrix $\mathcal{B}$. The corresponding uncertainty sets S_k are then defined by:

$$S_k(k) \coloneqq \textstyle\sum_{i=1}^{k-1} A_k^i\ \overline{\mathbb{W}} = \overline{\mathbb{W}} \oplus A_k^1\overline{\mathbb{W}} \oplus \dots \oplus A_k^{k-1}\overline{\mathbb{W}}, \tag{28}$$

where $\oplus$ denotes the set addition. Since A_k is stable, the set $S_k(\infty) \coloneqq \sum_{i=1}^{\infty} A_k^i\,\overline{\mathbb{W}}$ exists and is the positive invariant for $e(k+1) = A_K e(k) + \mathcal{W}$; furthermore, $S_k(i) \rightarrow S_k(\infty)$ is in the Hausdorff metric by $i \rightarrow \infty$. The above-mentioned procedure delivers the design for the ancillary controller. Consequently, $e(k+1) = A_k e(k) + \mathcal{W}$ is bounded according to Assumption 1. ∎

To achieve real-time properties, we linearised the nominal system at each sample time k to achieve a linear time-varying (LTV) model for prediction:

$$\bar{z}(k+1) = \frac{\partial(\mathcal{A}\,Z(k))}{\partial z}\,\bar{z}(k) + \frac{\partial(\mathcal{B})}{\partial u}u(k), \tag{29}$$

$$\begin{aligned} \bar{\mathcal{A}}|_k &\coloneqq \frac{\partial(\mathcal{A}\,Z(k))}{\partial z}, \\ \bar{\mathcal{B}}|_k &\coloneqq \frac{\partial(\mathcal{B}(z(k)))}{\partial u}, \\ \bar{z}(k) &= z(k), \end{aligned} \tag{30}$$

$$\bar{z}(k+1) = \bar{\mathcal{A}}|_k\bar{z}(k) + \bar{\mathcal{B}}|_k\,u(k). \tag{31}$$

Consequently, the system outputs are predicted as:

$$\bar{y}(k) = C\bar{z}(k), \tag{32}$$

where $C = [I \quad Z_o]$, I is the identity matrix, and Z_o is a zero matrix with proper dimensions. Consequently, the optimal problem of the proposed RMP-VDC is defined as:

$$\begin{aligned} &V(y,k) = \min_u\ J(\bar{y}, u, k) \\ &\text{Subject to:} \end{aligned} \tag{33}$$

$$\bar{z}(k+i+1) = \bar{\mathcal{A}}|_k\,\bar{z}(k+i) + \bar{\mathcal{B}}|_k\,u(k+i).\ i = 0, 1, 2, \dots, N-1, \tag{34}$$

$$\bar{y}(k+i) = \bar{z}(k+i), \tag{35}$$

$$|u(k+i)| \le u_{max}(k), \tag{36}$$

where $J(\bar{y}, u, k)$ is:

$$\begin{aligned} J(\bar{y}, u, k) &= \textstyle\sum_{i=1}^{N}\Big[\big(y_d(k+i|k) - \\ &\bar{y}(k+i|k)\big)^T Q_i(y_d(k+i|k) - \bar{y}(k+i|k)) + \\ &u\,(k+i-1|k)^T\,R_i u\,(k+i-1|k)\Big], \end{aligned} \tag{37}$$

where N is the prediction horizon, whereas $y_d(k+i|k)$ and $\bar{y}(k+i|k)$ represent the desired trajectory and the predicted system output for $i = 1, \dots, N$ at time k, respectively. The positive definite matrices Q_i and R_i are the designing weights for the tracking error and the control effort for $i = 1, \dots, N$, respectively.

The constraint u_{max} is considered as:

$$u_{max}(k) = u_{max} - K(k)e_{max} - {}^{s}F_r, \tag{38}$$

with:

$$e_{max} = \sup_{\mathcal{W}\in\overline{\mathbb{W}}} \mathcal{W}. \tag{39}$$

Therefore, the optimal control vector $U^*(k)$ is:

$$\begin{aligned} U^*(k) &\coloneqq \arg\min_u\ J(\bar{y}, u, k)\ \text{s.t. Eq.}\,(34)-(36))\} \\ &= [u^*(k|k), u^*(k+1|k), \dots, u^*(k+N-1|k)]^T, \end{aligned} \tag{40}$$

and control input is the first element of $U^*[k]$, $u^*(k|k)$, to apply to the system at $t = k\Delta t$. The analytically solution of the optimal problem with an active set method is obtained as in [10]. Consequently, the input signal of the proposed RMP-VDC shown in (6) for the system can be rewritten as:

$$\begin{aligned} {}^{s}F &= \hat{M}_s{}^{s}\dot{V}_r + \hat{C}_s{}^{s}V_r + \hat{G}_s + {}^{s}\overline{F}_r + K_s({}^{s}V_r - {}^{s}V) + \\ &u^*(k|k) + K(k)e(k). \end{aligned} \tag{41}$$

In summary, in this section, a new VDC method is presented based on the robust model predictor for a system with model uncertainties and interaction/external forces. The given mathematics of the proposed method is then used for implementation, which is presented in the following section.

IV. Experimental Results

In this section, the proposed RMP-VDC is experimentally implemented on a real 7-DoF upper body exoskeleton robot (ABLE). After placing a marker pen in the exoskeleton end-effector, the implementation test is then to draw a square with 10 cm sides on the whiteboard. Fig. 2 (a) depicts the real process of drawing this square by the exoskeleton robot. Moreover, for improved validation, the results of the proposed method are compared with the adaptive VDC method in [14]. The implemented control parameters of both control methods are given in Table I, which are selected after trial and error to achieve the best results.

The results of the implementation are demonstrated in Fig. 2 (b), Fig. 3 and Fig. 4. Fig. 2 (b) shows the desired and actual trajectories of the exoskeleton end-effector for the adaptive VDC and the proposed RMP-VDC. As shown in Fig. 2 (b), both controllers have stable performances; however, the performances were somewhat different. To better compare this difference, Fig. 3 (a) shows the desired and actual trajectory of the end-effector, while the error of each axis is depicted in Fig. 3 (b). For better validation, the outputs and tracking errors of each joint are depicted in Fig. 4 (a) and (b), respectively.

Additionally, mean square errors (MSEs), energy consumption (J_f) and performance indicator (ρ) are calculated to evaluate the performances of the control methods and numerical comparison. The normalising performance indicator (see [26] for additional details) and J_f are defined as:

$$\rho = \frac{\max(|\theta_{des} - \theta_a|)}{\max(|\dot{\theta}_a|)} = \frac{|e_\theta|_{max}}{|\dot{\theta}_a|_{max}}, \quad (42)$$

$$J_f = \frac{1}{T} \int_0^T |^sF|\, dt, \quad (43)$$

where θ_{des} and θ_a are the desired and actual positions, respectively, and $\dot{\theta}_a$ and T are actual velocity and total implementation time, respectively. TABLE II indicates the MSEs and ρ of the x-, y- and z-axes for the exoskeleton end-effector. In addition, the MSEs, ρ and J_f are calculated for each joint and are provided in TABLE III. The best results are shown in bold in TABLE II and TABLE III to facilitate reading. Furthermore, the comparative percentages of the methods are given under each numerical value.

In conclusion, as shown in TABLE II, the proposed controller performs better in all variables, meaning that it has lower MSEs and ρ compared with the adaptive VDC for the x-, y- and z-axes. In TABLE III, the results of most variables show that the performance of the proposed controller improved. For example, the J_f of all joints is highly optimal for the proposed RMP-VDC method, except for joint number 5, where the performance of the adaptive VDC improved by only 7%. Although the results show a considerable advantage for the adaptive VDC method in joint number 6, the overall end-effector performance is decidedly better with the proposed method. Therefore, the end-effector and joint results show the superiority of the proposed RMP-VDC method for the complex real 7-DoF exoskeleton robot, specifically when handling the model uncertainties, disturbances and interaction forces between humans and the robot.

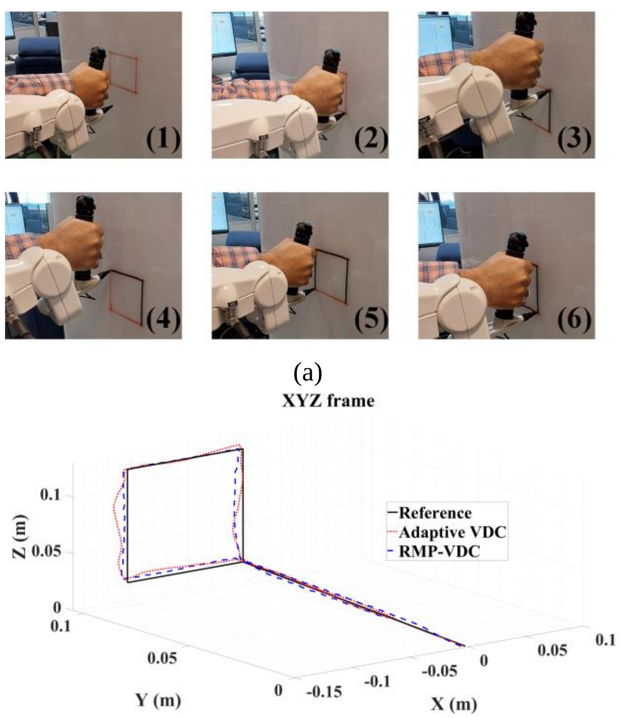

Figure 2. End-effector results. a) The real process of drawing a square by the exoskeleton robot and b) the desired and actual trajectories of the exoskeleton end-effector for adaptive VDC and the proposed RMP-VDC.

V. CONCLUSION

Here, we proposed a robust model predictive-based VDC method to tackle the inherent nonlinearity, model uncertainties and external disturbances for complex and high DoF robot manipulators by considering the input saturations. We first developed the VDC method based on a robust model predictor. The constraint optimal problem was then solved using the LTV approach to analytically calculate the ancillary controller of the prediction scheme and to provide the real-time controller. Consequently, the proposed controller was validated with implementation on a real 7-DoF arm exoskeleton robot, and the output results were compared with the adaptive VDC method. These experimental results reveal

TABLE I. CONTROL PARAMETERS OF ADAPTIVE VIRTUAL DECOMPOSITION CONTROL (VDC) AND THE PROPOSED ROBUST MODEL PREDICTIVE (RMP)-VDC FOR 7-DOF EXOSKELETON ROBOT

Controllers	Δt	α	K_s	Q	R	N
Adaptive VDC	1 ms	10	0.1	–	–	–
The proposed RMP-VDC	5 ms	10	0.01	10	0.1	5

TABLE II. MEAN SQUARE ERRORS (MSES) AND PERFORMANCE INDICATOR (ρ) OF X-, Y- AND Z-AXES FOR ADAPTIVE VIRTUAL DECOMPOSITION CONTROL (VDC) AND THE PROPOSED ROBUST MODEL PREDICTIVE (RMP)-VDC

Axis	*Adaptive VDC*		*The proposed Robust VD-based MPC*	
	MSE $\times 10^{-5}$	ρ $\times 10^{-3}$	MSE $\times 10^{-5}$	ρ $\times 10^{-3}$
X	1.92 (32%)	92.8 (63%)	**1.46 (0%)**	**56.9 (0%)**
Y	3.62 (96%)	87.8 (51%)	**1.84 (0%)**	**83.6 (0%)**
Z	2.18 (47%)	77.0 (202%)	**2.47 (0%)**	**25.5 (0%)**

TABLE III. MEAN SQUARE ERRORS (MSES), PERFORMANCE INDICATOR (ρ) AND ENERGY CONSUMPTION (J) OF EACH JOINT FOR ADAPTIVE VIRTUAL DECOMPOSITION CONTROL (VDC) AND THE PROPOSED ROBUST MODEL PREDICTIVE (RMP)-VDC

Joint	*Adaptive VDC*			*The Proposed Robust VD-based MPC*		
	MSE $\times 10^{-5}$	ρ $\times 10^{-3}$	J_f	MSE $\times 10^{-5}$	ρ $\times 10^{-3}$	J_f
#1	10.23 (267%)	84.1 (107%)	1.48 (11%)	**2.79 (0%)**	**40.6 (0%)**	**1.34 (0%)**
#2	7.74 (67%)	56.1 (18%)	1.32 (1%)	**4.63 (0%)**	**47.5 (0%)**	**1.31 (0%)**
#3	25.65 (168%)	**52.1 (0%)**	1.18 (34%)	**9.54 (0%)**	77.7 (49%)	**0.88 (0%)**
#4	**27.50 (0%)**	165.9 (280%)	1.08 (33%)	62.1 (125%)	**43.7 (0%)**	**0.81 (0%)**
#5	4.01 (7%)	35.8 (50%)	**0.26 (0%)**	**3.75 (0%)**	**24.0 (0%)**	0.27 (7%)
#6	**15.17 (0%)**	**23.3 (0%)**	0.21 (1%)	48.9 (223%)	98.1 (322%)	**0.20 (0%)**
#7	**4.56 (0%)**	39.2 (21%)	0.14 (76%)	5.45 (20%)	**32.4 (0%)**	**0.08 (0%)**

increased accuracy for the proposed RMP-VDC in dealing with interaction forces between humans and exoskeleton robots.

Hence, in the future, we will investigate the proposed RMP-VDC algorithms for highly complex systems, such as multi-robot manipulators and teleoperating master–slave systems [16]. Given that the proposed method enables optimal cooperation of multi-robot manipulators by considering the constraints of the environment and actuators, as well as handling the model uncertainties and external disturbances, it can be introduced in the control of multi-robot systems. Furthermore, equipping the VDC method with tools that benefit from the advantage of dynamic behaviour prediction can provide the required scaled forces for our dissimilar master and slave systems.

ACKNOWLEDGMENT

The TITAN (Teaching human-like abilities to heavy mobile machines through multisensory presence) project is funded by the Technology Industries of Finland Centennial Foundation and the Jane and Aatos Erkko Foundation Future Makers programme. 2020-2023 PI.

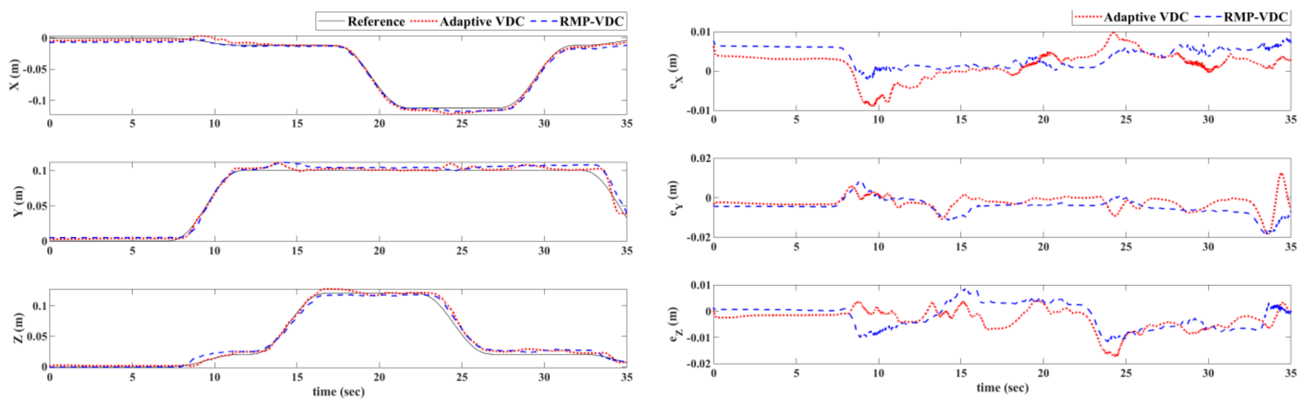

(a) (b)

Figure 3. End-effector results. a) The desired and actual trajectory of x-, y- and z-axes and b) tracking error for adaptive VDC and the proposed RMP-VDC.

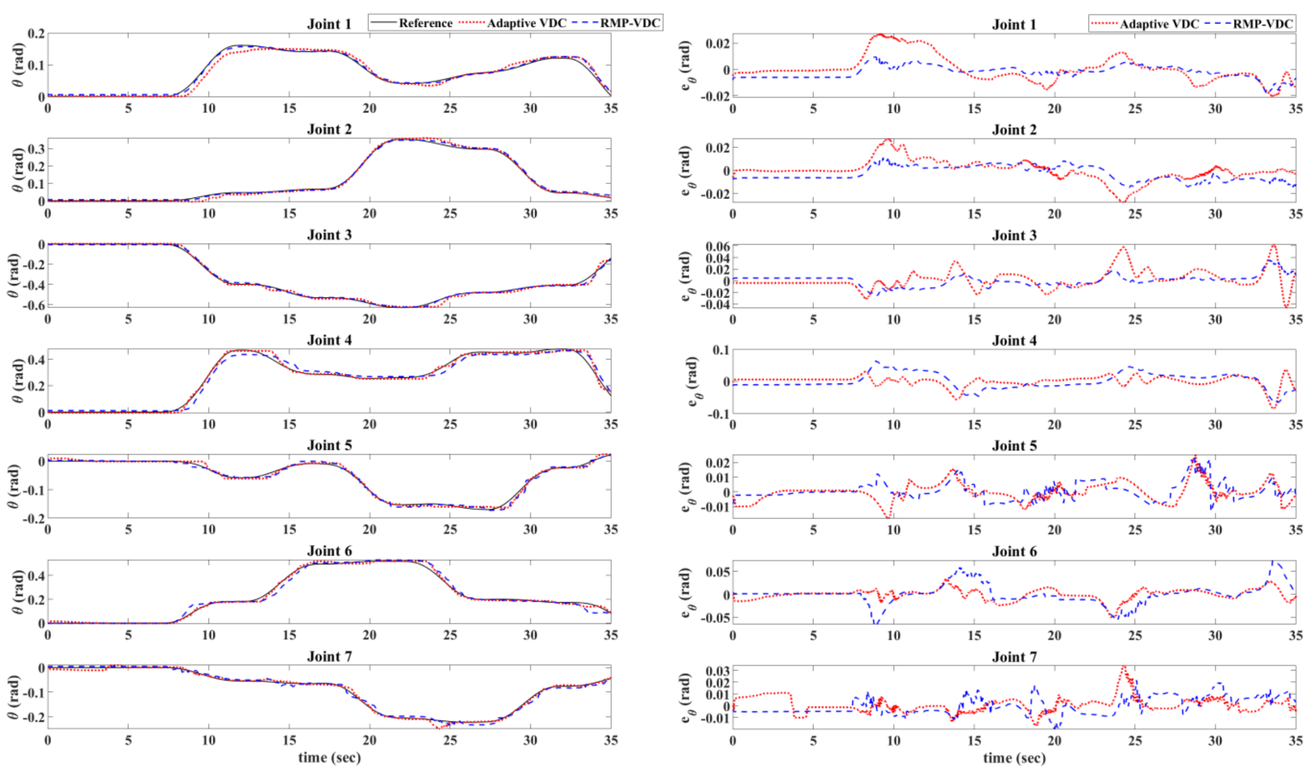

(a) (b)

Figure 4. Joint results. a) The desired and actual position of each joint and b) tracking error for adaptive VDC and the proposed RMP-VDC.

REFERENCES

[1] Z. Song, J. Yi, D. Zhao, and X. Li, "A computed torque controller for uncertain robotic manipulator systems," *Fuzzy Sets and Systems*, vol. 154, no. 2, pp. 208–226, 2005.

[2] M. K. Ciliz, "Adaptive control of robot manipulators with neural network-based compensation of frictional uncertainties," *Robotica*, vol. 23, no. 2, pp. 159–167, 2005.

[3] B. Brahmi, I. el Bojairami, T. Ahmed, M. H. Rahman, A. A. Z. Swapnil, and J. S. de Caro, "New Adaptive Sliding Mode for Unperturbed Forearm and Wrist Rehabilitation Robot," in *18th IEEE International Multi-Conference on Systems, Signals and Devices*, 2021, pp. 1160–1165.

[4] S. M. Tahamipour-Z., M.-R. Akbarzadeh-T., and F. Baghbani, "Interval type-2 generalized fuzzy hyperbolic modelling and control of nonlinear systems," *Applied Soft Computing*, vol. 123, 2022.

[5] M. G. Farajzadeh-D., S. K. Hosseini S., and A. Akbarzadeh, "Performance enhancement of model reference adaptive control through normalized Lyapunov design," *Proceedings of the Institution of Mechanical Engineers. Part I: Journal of Systems and Control Engineering*, vol. 233, no. 9, pp. 1209–1220, 2019.

[6] M. H. Rahman, K. Kiguchi, Md. M. Rahman, and M. Sasaki. "Robotic exoskeleton for rehabilitation and motion assist." in *First IEEE International Conference on Industrial and Information Systems*, 2006, pp. 241-246.

[7] E. A. Brackbill, Y. Mao, S. K. Agrawal, M. Annapragada, and V. N. Dubey, "Dynamics and control of a 4-dof wearable cable-driven upper arm exoskeleton," in *Proceedings - IEEE International Conference on Robotics and Automation*, 2009, pp. 2300–2305.

[8] I. Kardan and A. Akbarzadeh, "Robust output feedback assistive control of a compliantly actuated knee exoskeleton," *Robotics and Autonomous Systems*, vol. 98, pp. 15–29, 2017.

[9] N. Naghavi, A. Akbarzadeh, S. M. Tahamipour-Z., and I. Kardan, "Assist-As-Needed control of a hip exoskeleton based on a novel strength index," *Robotics and Autonomous Systems*, vol. 134, 2020.

[10] S. M. Tahamipour-Z., S. K. Hosseini-S., M. R. Akbarzadeh-T., A. Akbarzadeh, and M.-G. Farajzadeh-D., "Design and Implementation of a Real-Time Nonlinear Model Predictive Controller for a Lower Limb Exoskeleton with Input Saturation," *Iranian Journal of Science and Technology - Transactions of Electrical Engineering*, vol. 45, no. 1, 2021.

[11] M. R. Islam, B. Brahmi, T. Ahmed, Md. Assad-Uz-Zaman, and M. H. Rahman, "Exoskeletons in upper limb rehabilitation: A review to find key challenges to improve functionality," *Control Theory in Biomedical Engineering*, Elsevier, 2020.

[12] B. Brahmi, M. Saad, C. Ochoa-Luna, M. H. Rahman, and A. Brahmi, "Adaptive Tracking Control of an Exoskeleton Robot with Uncertain Dynamics Based on Estimated Time-Delay Control," *IEEE/ASME Transactions on Mechatronics*, vol. 23, no. 2, pp. 575–585, 2018.

[13] B. Brahmi, M. Driscoll, I. K. el Bojairami, M. Saad, and A. Brahmi, "Novel adaptive impedance control for exoskeleton robot for rehabilitation using a nonlinear time-delay disturbance observer," *ISA Transactions*, vol. 108, pp. 381–392, 2021.

[14] W. H. Zhu, "Virtual Decomposition Control-Toward Hyper Degrees of Freedom Robots," vol. 10. Berlin: Springer, 2010.

[15] S. Lampinen, J. Koivumaki, W. H. Zhu, and J. Mattila, "Force-Sensor-Less Bilateral Teleoperation Control of Dissimilar Master-Slave System with Arbitrary Scaling," *IEEE Transactions on Control Systems Technology*, vol. 30, no. 3, pp. 1037–1051, 2022.

[16] J. Koivumäki, W. H. Zhu, and J. Mattila, "Energy-efficient and high-precision control of hydraulic robots," *Control Engineering Practice*, vol. 85, pp. 176–193, 2019.

[17] G. R. Petrović and J. Mattila, "Mathematical modelling and virtual decomposition control of heavy-duty parallel–serial hydraulic manipulators," *Mechanism and Machine Theory*, vol. 170, 2022.

[18] S. Mastellone and A. van Delft, "The impact of control research on industrial innovation: What would it take to make it happen?," *Control Engineering Practice*, vol. 111, 2021.

[19] C. Ochoa Luna, M. H. Rahman, M. Saad, P. Archambault, and W. H. Zhu, "Virtual decomposition control of an exoskeleton robot arm," *Robotica*, vol. 34, no. 7, pp. 1587–1609, 2016.

[20] D. Q. Mayne, "Model predictive control: Recent developments and future promise," *Automatica*, vol. 50, no. 12, pp. 2967–2986, 2014.

[21] T. Ding, Y. Zhang, G. Ma, Z. Cao, X. Zhao, and B. Tao, "Trajectory tracking of redundantly actuated mobile robot by MPC velocity control under steering strategy constraint," *Mechatronics*, vol. 84, 2022.

[22] A. K. Kashyap and D. R. Parhi, "Optimization of stability of humanoid robot NAO using ant colony optimization tuned MPC controller for uneven path," *Soft Computing*, vol. 25, no. 7, pp. 5131–5150, Apr. 2021.

[23] M. G. Farajzadeh-D. and S. K. H. Sani, "An improved two-loop model predictive control design for nonlinear robust reference tracking with practical advantages," *Optimal Control Applications and Methods*, vol. 42, no. 2, pp. 548–565, 2021.

[24] A. Liu, W.-A. Zhang, and L. Yu, "Robust Predictive Tracking Control for Mobile Robots with Intermittent Measurement and Quantization," *IEEE Transactions on Industrial Electronics*, vol. 68, no. 1, pp. 509–518, 2020.

[25] F. M. Smaldone, N. Scianca, V. Modugno, L. Lanari, and G. Oriolo, "ZMP Constraint Restriction for Robust Gait Generation in Humanoids," in *IEEE International Conference on Robotics and Automation (ICRA)*, 2020, pp. 8739-8745.

[26] W. H. Zhu, T. Lamarche, E. Dupuis, D. Jameux, P. Barnard, and G. Liu, "Precision control of modular robot manipulators: The vdc approach with embedded fpga," *IEEE Transactions on Robotics*, vol. 29, no. 5, pp. 1162–1179, 2013.